# Nonlinear rheological behavior of bitumen under LAOS stress

Liyan Shan*
School of Transportation Science and Engineering, Harbin Institute of Technology, Harbin, Heilongjiang, China, 150090
Hongsen He
School of Transportation Science and Engineering, Harbin Institute of Technology, Harbin, Heilongjiang, China, 150090
Norman J. Wagner
Center for Molecular and Engineering Thermodynamics, Department of Chemical and Biomolecular Engineering, University of Delaware, Newark, Delaware, 19716
Zhuang Li
School of Transportation Science and Engineering, Harbin Institute of Technology, Harbin, Heilongjiang, China, 150090

Synopsis

The linear viscoelasticity and steady shear properties of bitumen are established, however, bitumen used in pavement also supports time-varying loading in the nonlinear regime. Consequently, recent research focuses on the nonlinear rheological behavior of bitumen under time-varying flows that is essential for establishing the constitutive model. Here we propose a protocol to obtain the nonlinear rheological behavior of bitumen from such as under large amplitude oscillatory shear stress (LAOS stress). The LAOS stress rheological response of both a neat bitumen and a modified bitumen are analyzed by FT-rheology and strain decomposition to an orthogonal set of Chebyshev polynomials. We find that the relative nonlinearity of bitumen increases with increase in stress and decrease in frequency; the relationship between $I_3/I_1$ and stress amplitude can obey the sigmoidal function; the intrinsic nonlinearity $Q_0$ decreases with increase in frequency and decrease in temperature. Both the FT analysis results and decomposition results show that the nonlinearity of modified bitumen B is much more significant than neat bitumen A. Bitumen A exhibits stress softening and stress thinning under all the studied test conditions, but bitumen B exhibits stress stiffening under some conditions.

## Ⅰ. INTRODUCTION

The rheological behavior of bitumen has always been of critical interest to paving technologists because it is linked to the in-service behavior of actual bituminous pavements. The rheological behavior of bitumen can be measured under both steady-state shear for its creep, relaxation or viscosity properties [1-4] and oscillatory shear for its dynamic rheological properties [5-9]. The bituminous pavement is believed to support oscillatory shear under traffic loading [10], so it is very important to obtain the dynamic rheological properties of the bituminous materials. Application of the time-temperature

superposition principle (TTSP) yields master curves for the modulus or phase angle [7,8,11,12]. The WLF equation [13] and Arrhenius [14] equations are empirically employed to create master curves, enabling predictions of some rheological properties of bitumen over a wider frequency and temperature range. Differences between bitumen variants and the effects of additives as well as aging on the rheological behavior can be identified by comparing such master curves [9,15].

Based on these limited rheological measurements, different kinds of constitutive equations have been proposed to describe the rheological behavior of bitumen. Some models used the glassy modulus, frequency at glassy modulus, together with a shape parameter to describe the master curve [16,17]. Other models utilized physical elements to describe the viscoelastic behavior of bitumen, such as generalized Maxwell, Burgers, generalized Kelvin, Huet–Sayegh and DBN model, etc. [18-24].

All the abovementioned literatures are concerned with the linear viscoelastic behavior of bitumen. However, bitumen will undergo large loadings during its service life, which results in nonlinear deformation that can be quasi-periodic in time [25]. Rheological tests using LAOS have been proposed for studying construction materials, such as cements [26]. LAOS is a powerful method to independently measure rate or frequency effects independent of amplitude, and a number of methods have been proposed to interpret the results [27-29]. Consequently, there is a recent interest in the nonlinear rheological behavior of bitumen under large amplitude oscillatory shear (LAOS). For example, Padmarehka et al. studied the linear and nonlinear behavior of three different kinds of bitumen, and established a frame invariant nonlinear constitutive model [30]. Farrar et al. showed that the elasticity appeared dominant when the strain amplitude was less than 30% [31]. Jorshari et al. measured the nonlinear rheological behavior of SBS modified bitumen under LAOS and compared the first, the third and the fifth harmonic moduli [32, 33]. González et al. tested the rheological characterization of neat bitumen and EVA, HDPE polymer modified bitumen with the LAOS-FTR method, and showed that polymer modified bitumen exhibits higher harmonics ($I_n/I_1$ with $3 \leq n \leq 9$), such that this method could quantitatively differentiate between the tested binders [34].

While these works demonstrate that there is value in LAOS studies on bitumen, many aspects remain unexplored, such as the standard test and analysis method are not established and the mechanical behaviors under LAOS were not clear. Importantly, as a road construction material, bitumen is definitely going to bear time-varying stress controlled loading. In the field of road engineering, the common practice is to employ controlled strain tests for bitumen materials used in thin pavement and controlled stress tests for bitumen materials used in thick pavement [35]. Differences are noted between LAOS strain versus stress experiments on complex fluids [36]. Ewoldt and co-workers have proposed a method for analysis of LAOS stress experiments [37]. Consequently, it is necessary and important to study the rheological behavior of bitumen under LAOS stress, which is the novelty of the work presented here.

The goal of this work is to explore the nonlinear rheological behavior of bitumen

under LAOS stress. In the following, we specify a protocol to measure the bitumen behavior under LAOS stress for a neat bitumen and a modified bitumen at various frequencies and stress amplitudes. The nonlinearity ($I_3/I_1$) from FT-rheology as a function of stress amplitude was investigated as a material metric. The dynamic strain was decomposed into elastic and viscous contributions. The Lissajous plots with the decomposed elastic/viscous strain at different stress levels were analyzed to investigate the stress thinning/thickening and stress softening/stiffening behavior as a function of stress level.

## Ⅱ. MATERIALS AND METHODS

### A. Materials

One neat bitumen and one bitumen modified with SBS (Styrene-Butadiene-Styrene) and crumb rubber were selected for this study. The SBS is linear and the content is about 4.25 percent by weight. They are identified as bitumen A and bitumen B, respectively. The PG grade of bitumen A is PG64-22, and the PG grade of bitumen B is PG76-22. Based on the PG grading specification, the nomenclature of PG64-22 bitumen means that the bitumen is suitable for the area where the highest temperature (average maximal temperature in 7 days) is lower than 64°C and the lowest temperature is higher than -22°C. PG76-22 bitumen means that the bitumen is suitable for the area where the highest temperature (average maximal temperature in 7 days) is lower than 76°C and the lowest temperature is higher than -22°C. The components of these two types of bitumen are shown in Table Ⅰ. In the component theory of bitumen, the bitumen can be envisioned to be composed of asphaltene, resin, saturate and aromatic (SARA for short). Bitumen has a colloidal structure where the asphaltenes stabilized by resin are generally considered to be the dispersed phase, with the mixture of saturate plus aromatics acting as the dispersing medium phase [38]. Consequently, bitumen with higher percentage of dispersed phase is stiffer than the one with lower percentage of dispersed phase [39,40]. Based on this and the compositions listed in Table Ⅰ, it is anticipated that bitumen B is stiffer than bitumen A, which will also be shown in the following section.

**TABLE Ⅰ**. Components of the studied bitumens.

| Bitumen type | Component (%) | | | |
|---|---|---|---|---|
| | Asphaltene | Resin | Saturate | Aromatics |
| A | 13.93 | 27.24 | 28.31 | 30.52 |
| B | 17.66 | 25.96 | 31.82 | 24.56 |

The SAOS master curves of the studied bitumen are shown in Figure.1. It can be seen from Figure 1(a) and 1(b) that the loss modulus is greater than the storage modulus for bitumen A and B in the studied frequency range (≤60rad/s) at both 30°C and 60°C. It means that the viscous part is large than the elastic part for the studied bitumen under the research test conditions, which is typical of suspensions [41]. The generalized Kelvin

model (shown in Eq.(1)) was used to fit the tested modulus data, and the fitting results are also shown in Figure 1 (A table of the parameter values is provided in the Supplemental Material). As expected, the model can well describe the storage and loss modulus. These fitting results further prove our previous study that the generalized Kelvin model can well describe the modulus and phase angle if n is large enough [42]. Figure 1(c) shows that the shift factors for the different bitumens are similar to each other at the same temperature. Besides that, it can be seen from Figure 1(a) and 1(b) that there is no plateau in the master curve when the reduced frequency is small, which is different from most colloidal materials. The highest temperature used to test the bitumen is usually the temperature corresponding to the high PG grade (for example 64°C for bitumen A) and it is meaningless to test the bitumen at very high temperature. So there is no plateau in the low frequency range by using the common used temperature range. The shapes of the master curve in Figure 1(a) and 1(b) are similar to the bitumen master curves in the published literatures.

$$G'(\omega) = \sum_{i=1}^{n} \frac{G_i}{G_i^2 + \eta_i^2 \omega^2} + \frac{1}{G_0}, \qquad G''(\omega) = \sum_{i=1}^{n} \frac{\eta_i \omega}{G_i^2 + \eta_i^2 \omega^2} + \frac{1}{\eta_0 \omega} \tag{1}$$

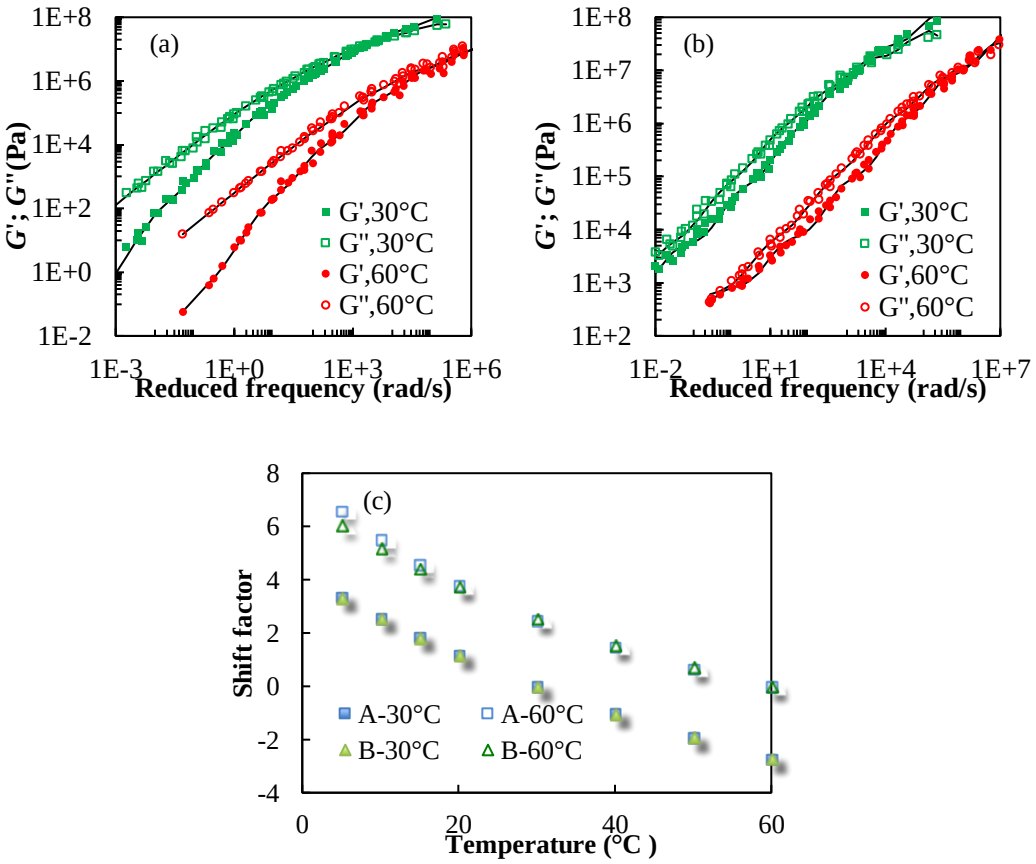


**FIG.1.** Dynamic shear moduli for (a) bitumen A and (b) bitumen B, and the

corresponding shift factors (c). Data were collected at different temperatures and shifted in frequency to a reference state of 30 and 60ºC. These two temperatures were used for the LAOS tests. Lines were calculated from G(t) using Eq. (1). G' are indicated with closed and G" with open symbols. The shift factors were fit to the WFL equation.

The steady shear viscosity of bitumen A and B at 30°C and 60°C are shown in Figure 2. In contrast with more traditional colloidal suspensions, it is difficult to obtain the infinite shear viscosity of bitumen by shear rheometer. As expected, the bitumen viscosity at 30°C is greater than that at 60°C. The viscosity of bitumen B is greater than that of bitumen A at both 30°C and 60°C, such that bitumen B is stiffer than bitumen A as expected from the bitumen components given in Table Ⅰ.

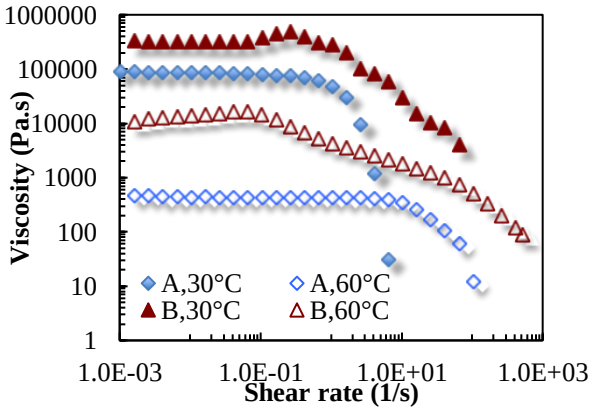


**FIG.2.** Viscosity curves of the studied bitumens

**B. Rheological measurements**

The rheological behavior of the bitumen was tested using a TA Instruments ARG-2 stress controlled rheometer operated in native mode using disposable fixtures and the oven for temperature control. The tests were conducted with an 8-mm diameter parallel plate geometry and 2-mm gap setting at 30°C, and with a 25-mm diameter parallel plate geometry and 1-mm gap setting at 60°C. After placed between the two plates, pressed to the trim gap and trimmed, the bitumen sample was heated to its high temperature grade (64 °C for bitumen A and 76 °C for bitumen B) for five minutes to let it adhere firmly to the plates. Then the temperature was lower to the test temperature and hold for 25 minutes before test. This procedure was to avoid the slip issue between the sample and the plates. In order to make sure the slip issue was avoided, the bonding condition between the sample and plates was checked carefully after each test. If this phenomenon happened, the data would be deleted and a new sample would be tested again. The frequency series were chosen as 1 rad/s, 2 rad/s, 5 rad/s, 10 rad/s and 60 rad/s. Stress sweep tests were conducted at each temperature and frequency to choose the stress levels for the oscillatory shear test. At least two replicates were done for each test condition, and the mean values and errors bars are displayed in Figure 3 and Figure 4. As shown in

Figure 3, the loss modulus is greater than the storage modulus, which illustrates that the bitumen behaves as a viscous suspension. For all bitumen samples at both 30 and 60°C, a significant linear regime is found. Bitumen A exhibits a near catastrophic failure at a critical stress amplitude at 30°C, such that the samples is visibly broken. Increasing the temperature leads to a more plastic response, but with a lower critical stress amplitude. The modified bitumen B exhibits a similar range of linearity, but is less "brittle" at 30°C than bitumen A. A significant difference is observed for the modified bitumen B at 60°C, where stress hardening is observed prior to material failure for the lower frequencies. These features and differences will be manifest in the LAOS results.

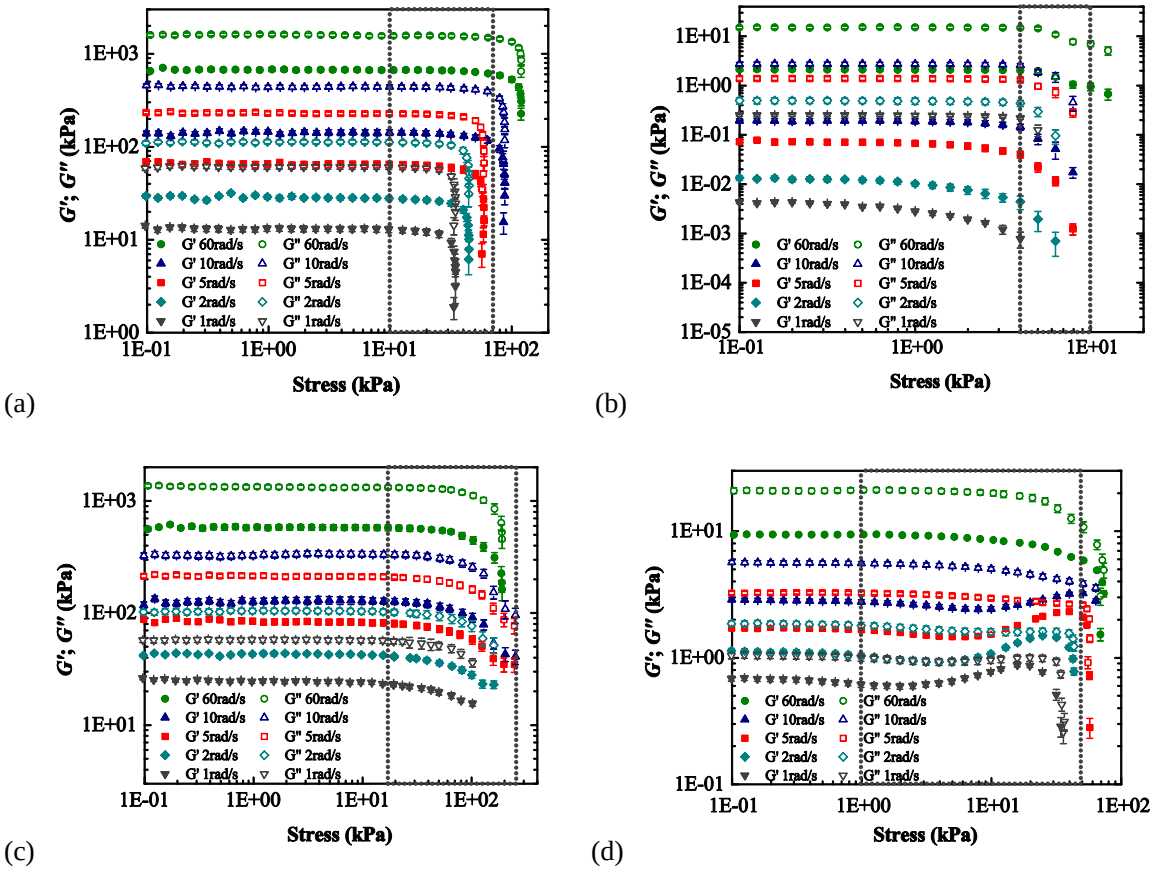


**FIG.3.** Stress sweep test results of the bitumen: (a) Bitumen A at 30°C; (b) Bitumen A at 60°C; (c) Bitumen B at 30°C; (d) Bitumen B at 60°C.

To test the bitumen at both linear range and nonlinear range at each frequency and temperature, the stress levels were chosen in the range between the two dotted lines, as shown in Figure 3. All the stress levels are summarized in Table Ⅱ and Table Ⅲ. "L" in the tables means that the stress level is in the linear range, meanwhile "N" in the tables means that the stress level is in the nonlinear range. Because the stress level the bitumen B can support is much larger than that of bitumen A, it is impossible to select the same

stress levels for the two bitumen at all the test conditions if we want to study the nonlinear rheological behavior. It is still reasonable to compare the nonlinearity of the two bitumens using the stress levels in Table Ⅱ, because the positions of the selected stress in the stress sweep curve between different bitumens are much similar to each other. For example, 70 kPa is almost the largest stress that bitumen A can support at 30°C, 260kPa is almost the largest stress that bitumen B can support at 30°C. So the nonlinearity degrees of the two bitumens could be compared indirectly.

**TABLE Ⅱ.** Selected stress levels of bitumen A.

| Frequency | Stress at 30 °C (kPa) | | | | | | | Stress at 60 °C (kPa) | | | | | | |
|---|---|---|---|---|---|---|---|---|---|---|---|---|---|---|
| (rad/s) | 10 | 20 | 30 | 40 | 50 | 60 | 70 | 4 | 5 | 6 | 7 | 8 | 9 | 10 |
| 1 | L | N | N | N | N | N | N | N | N | N | N | N | N | N |
| 2 | L | L | N | N | N | N | N | N | N | N | N | N | N | N |
| 5 | L | L | L | N | N | N | N | N | N | N | N | N | N | N |
| 10 | L | L | L | L | N | N | N | L | N | N | N | N | N | N |
| 60 | L | L | L | L | L | N | N | L | N | N | N | N | N | N |

**TABLE Ⅲ.** Selected stress levels of bitumen B.

| Frequency | Stress at 30 °C (kPa) | | | | | | | Stress at 60 °C (kPa) | | | | | | |
|---|---|---|---|---|---|---|---|---|---|---|---|---|---|---|
| (rad/s) | 20 | 60 | 100 | 140 | 180 | 220 | 260 | 1 | 5 | 10 | 20 | 30 | 40 | 50 |
| 1 | N | N | N | N | N | N | N | N | N | N | N | N | N | N |
| 2 | N | N | N | N | N | N | N | N | N | N | N | N | N | N |
| 5 | L | N | N | N | N | N | N | L | N | N | N | N | N | N |
| 10 | L | L | N | N | N | N | N | L | N | N | N | N | N | N |
| 60 | L | L | L | N | N | N | N | L | L | L | N | N | N | N |

Note: L means that this stress level is in linear range and N stands for nonlinear range.

### C. Data selection method

The LAOS stress responses of these materials were observed to be time-dependent, as shown for some select conditions in Figure 4. As noted by Ewoldt and co-workers [43] the LAOS can yield a drift in the average strain/stress, which is observed in Figure 4 and tabulated in the appendix. Further, the LAOS stress response evolves with cycling to a time-stable regime, which was identified for each condition as indicated in Figure 4. This time-stable oscillatory response is termed alternance. Note that continued oscillation will lead to material failure, as illustrated in Figure 4. The cycles used to analyze the nonlinear rheological behavior were selected at the steady phase where the modulus is around 85% of the initial dynamic modulus. Based on the former study, there should be no failure in the sample under this condition.

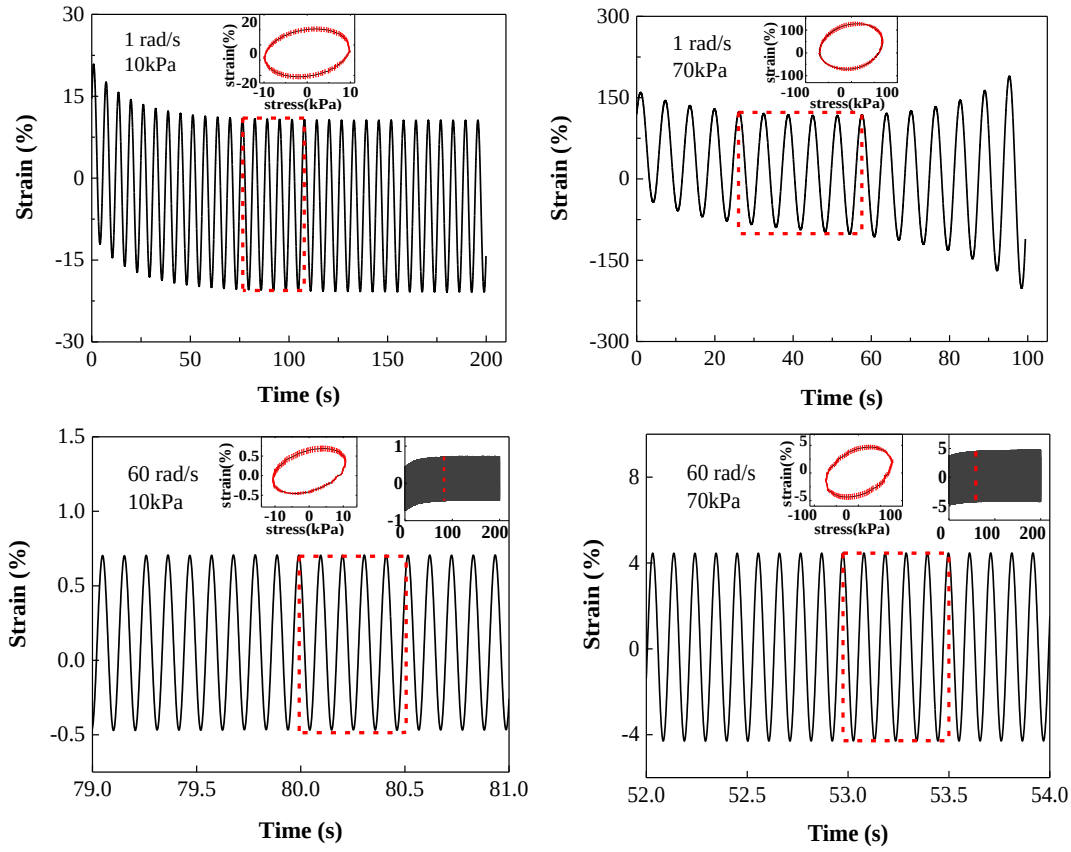
1 rad/s
10kPa
strain(%)
stress(kPa)
Strain (%)
Time (s)
1 rad/s
70kPa
60 rad/s
10kPa
60 rad/s
70kPa

(a) 30 ℃

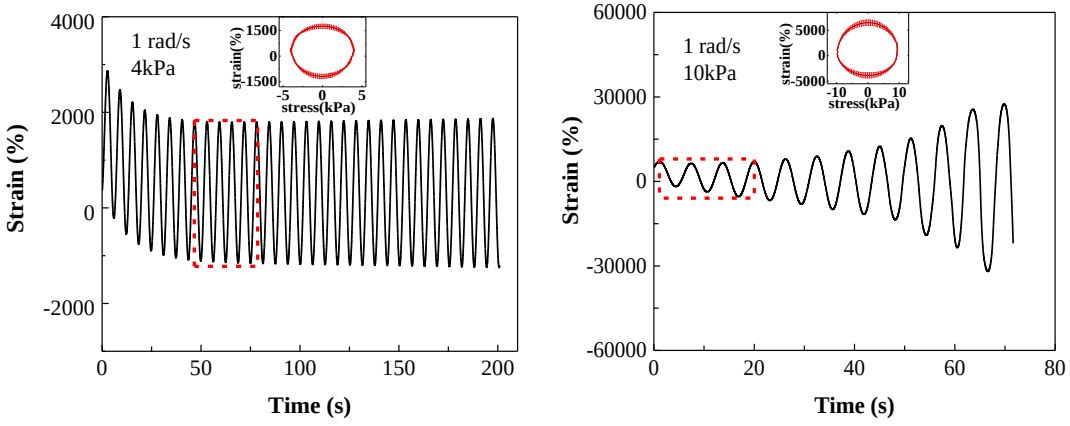
1 rad/s
4kPa
strain(%)
stress(kPa)
Strain (%)
Time (s)
1 rad/s
10kPa

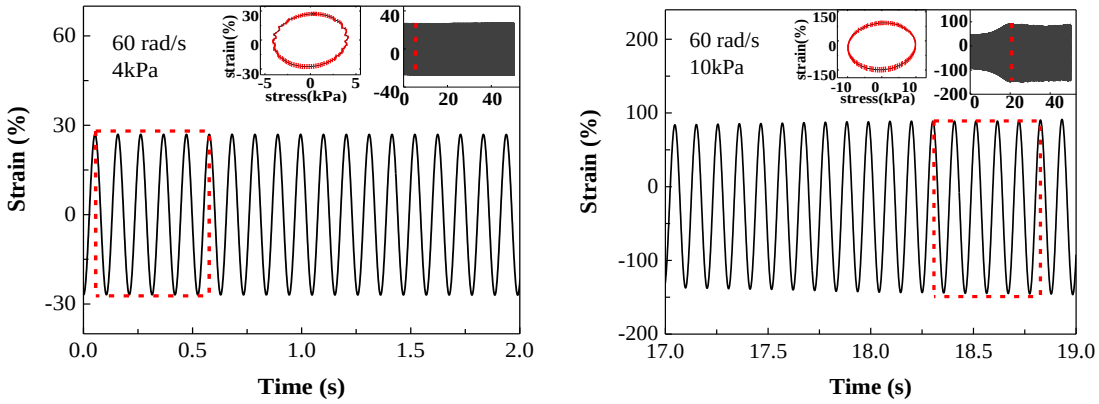


(b) 60 °C

**FIG. 4.** Strain response of bitumen A at (a) 30°C and (b) 60°C. The marked time regime is identified as the alternance state and used for further analysis.

### D. Data pre-treatment method

The strain-stress waveform obtained by the rheometer is shifted to zero average strain prior to analysis, as shown in Figure 5. All the shifting factors are summarized in the appendix.

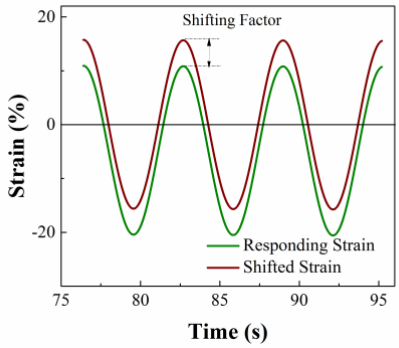


**FIG. 5.** Schematic of the waveform shift.

## Ⅲ. Theory

### A. FT-rheology

The theoretical aspects of FT-rheology are documented in more detail elsewhere [44-46]. Therefore, only the most pertinent mathematical relations are repeated here. The input shear stress is represented using cosine function, as shown in Eq.(2).

$$\sigma(t) = \sigma_0 \cos \omega t \tag{2}$$

The nonlinear shear strain response under LAOS stress can be expressed using a Fourier series expansion with either strain amplitude or stress amplitude with odd higher terms as follows [47].

$$\gamma(t) = \sum_{n=1,odd} \gamma_n \cos(n\omega t - \delta_n) \tag{3}$$

$$\gamma(t) = \sum_{n\ odd} \left\{ J_n'(\omega, \sigma_0)\sigma_0 \cos n\omega t + J_n''(\omega, \sigma_0)\sigma_0 \sin n\omega t \right\} \tag{4}$$

Symmetry shows that the shear strain curve contains only odd higher harmonic contributions under LAOS flow. FT-rheology decomposes the shear strain in the time domain into the frequency domain.

From Eq.(3), the shear strain from nonlinear oscillatory shear flow by FT-rheology can be described as

$$\gamma(t) = \gamma_1 cos(\omega t - \delta_1) + \gamma_3 cos(3\omega t - \delta_3) + \gamma_5 cos(5\omega t - \delta_5) + \cdots$$
$$= \gamma_1 \cos\delta_1 \cos\omega t + \gamma_1 \sin\delta_1 \sin\omega t + \gamma_3 \cos\delta_3 \cos 3\omega t + \gamma_3 \cos\delta_3 \cos 3\omega t + \cdots \quad (5)$$

From the above equation, the relative intensity of higher-harmonics [$I(n\omega)/I(\omega) = I_n/I_1$, where $\omega$ is the excitation frequency] from FT-rheolgy can be calculated as follows:

$$I_3/I_1 = \frac{\gamma_3}{\gamma_1} = \frac{\sqrt{(\gamma_3 \cos\delta_3)^2 + (\gamma_3 \sin\delta_3)^2}}{\sqrt{(\gamma_1 \cos\delta_1)^2 + (\gamma_1 \sin\delta_1)^2}}$$

$$I_5/I_1 = \frac{\gamma_5}{\gamma_1} = \frac{\sqrt{(\gamma_5 \cos\delta_5)^2 + (\gamma_5 \sin\delta_5)^2}}{\sqrt{(\gamma_1 \cos\delta_1)^2 + (\gamma_1 \sin\delta_1)^2}}$$

.....

(6)

Any measured response from the tested system at frequencies other than $\omega$ is associated with nonlinearity in the system response. Therefore, the relative intensity $I_n/I_1$ is usually used to evaluate the degree of non-linearity of the material's response.

The ratio of $I_3/I_1$ is the most common index used by the FT-rheology method. In a log-log plot, the ratio of $I_3/I_1$ shows a linear relationship with strain amplitude at small and medium strain amplitude, expressed as Eq.(7) [47,48]. Some researchers focused on analyzing the intercept "a" and slope "b", where they observed that the slope b equals two [49-51], as expected from the theory in the limit of small amplitudes. However, at large strain amplitude, Wilhelm and co-workers showed that $I_3/I_1$ is often observed to be a sigmoidal function that can empirically be described via Eq.(8) [52]. In bitumen research, there is no prior report on the functionality of $I_3/I_1$.

$$log(I_3/I_1) = a + b log\gamma_0 \quad (7)$$

$$I_3/I_1\,(\gamma_0) = A\left(1 - \frac{1}{1+(B\gamma_0)^C}\right) \quad (8)$$

**B. Strain decomposition method**

FT-rheology can quantify the degree of nonlinearity of the shear strain response, but the higher harmonics cannot provide all information about the nonlinear response. Therefore, the total strain is also analyzed with strain decomposition method. The viscoelastic strain measured in dynamic oscillatory shear flow can be decomposed into elastic and viscous parts in the linear regime. In the nonlinear regime, using the Fourier series representation of the strain signal represented in Eq.(4), the nonlinear strain can be

decomposed into an apparent elastic strain, $\gamma'$, and an apparent plastic strain, $\gamma''$[37]:

$$\gamma'(t) = \sigma_0 \sum_{n\,odd} J_n'(\omega, \sigma_0) \cos n\omega t \quad (9)$$

$$\gamma''(t) = \sigma_0 \sum_{n\,odd} J_n''(\omega, \sigma_0) \sin n\omega t \quad (10)$$

The strain decomposition is based on the idea that we desire $\gamma'$ and $\gamma''$, such that over one cycle of oscillation $\gamma'$ is a single-valued function of $\sigma$ and the apparent plastic strain rate $\dot{\gamma}''$ is a single-valued function of $\sigma$. The convention of naming $\gamma'$ an elastic strain and naming $\gamma''$ a plastic strain then follows because elastic strain typically depends only on imposed stress.

Following the reference of Ewoldt et al.(2008) [53] and Dimitriou et al. (2013)[37], The elastic strain and plastic strain can also be represented as a series of orthogonal Chebyshev polynomials $T_n(x)$, where $x$ is the scaled stress, $x = \sigma(t)/\sigma_0$:

$$\gamma'(t) = \sigma_0 \sum_{n\,odd} J_n'(\omega, \sigma_0) \cos n\omega t = \sigma_0 \sum_{n\,odd} \underbrace{J_n'(\omega, \sigma_0)}_{c_n} T_n(x) \quad (11)$$

$$\dot{\gamma}''(t) = \sigma_0 \sum_{n\,odd} n\omega J_n''(\omega, \sigma_0) \cos n\omega t = \sigma_0 \sum_{n\,odd} \underbrace{n\omega J_n''(\omega, \sigma_0)}_{f_n} T_n(x) \quad (12)$$

The above representation follows from the identity $T_n(\cos\theta) = \cos n\theta$. The resulting material coefficients in Eq. (11) and (12) have units consistent with compliances $c_n(\omega, \sigma_0)$ [Pa]$^{-1}$ and fluidities $f_n(\omega, \sigma_0)$ [Pa.s]$^{-1}$, respectively. The Fourier coefficient can represent a complete mathematical description of the time-domain response, but the physical interpretation of the higher harmonics is revealed by considering the Chebyshev coefficients in the orthogonal space formed by the input stress/stain and strain-rate [53-55].

## Ⅳ. RESULTS AND DISCUSSION

In this section, the nonlinear strains under LAOS stress for bitumen A and bitumen B were investigated using FT-rheology and stress decomposition method.

### A. FT-rheology analysis

When the stress amplitude is small such that the sample is in the linear oscillatory shear regime, the strain is sinusoidal. Increasing the stress amplitude results in a nonlinear response such that the strain is no longer sinusoidal and has higher harmonic contributions. FT-rheology shows that the higher harmonics $I_n/I_1$ becomes significant and increases with the stress amplitude, as shown in Figure 6 and Figure 7. For bitumen A, only $I_3/I_1$ and $I_5/I_1$ are measurable and they increase as the stress amplitude increases. However, for bitumen B, $I_7/I_1$ and $I_9/I_1$ are also measurable along with $I_3/I_1$ and $I_5/I_1$, and all of them increase as the stress amplitude increases. As bitumen A is neat and bitumen B is modified, these results also show that the nonlinearity of modified bitumen is much

more significant than neat bitumen at the test conditions explored. Note that there may be even peak in the Fourier spectra curve when the stress is very high. By analyzing the Fourier spectra of the input stress, it is found that the even peak appears because of the nonlinearity of the input signal.

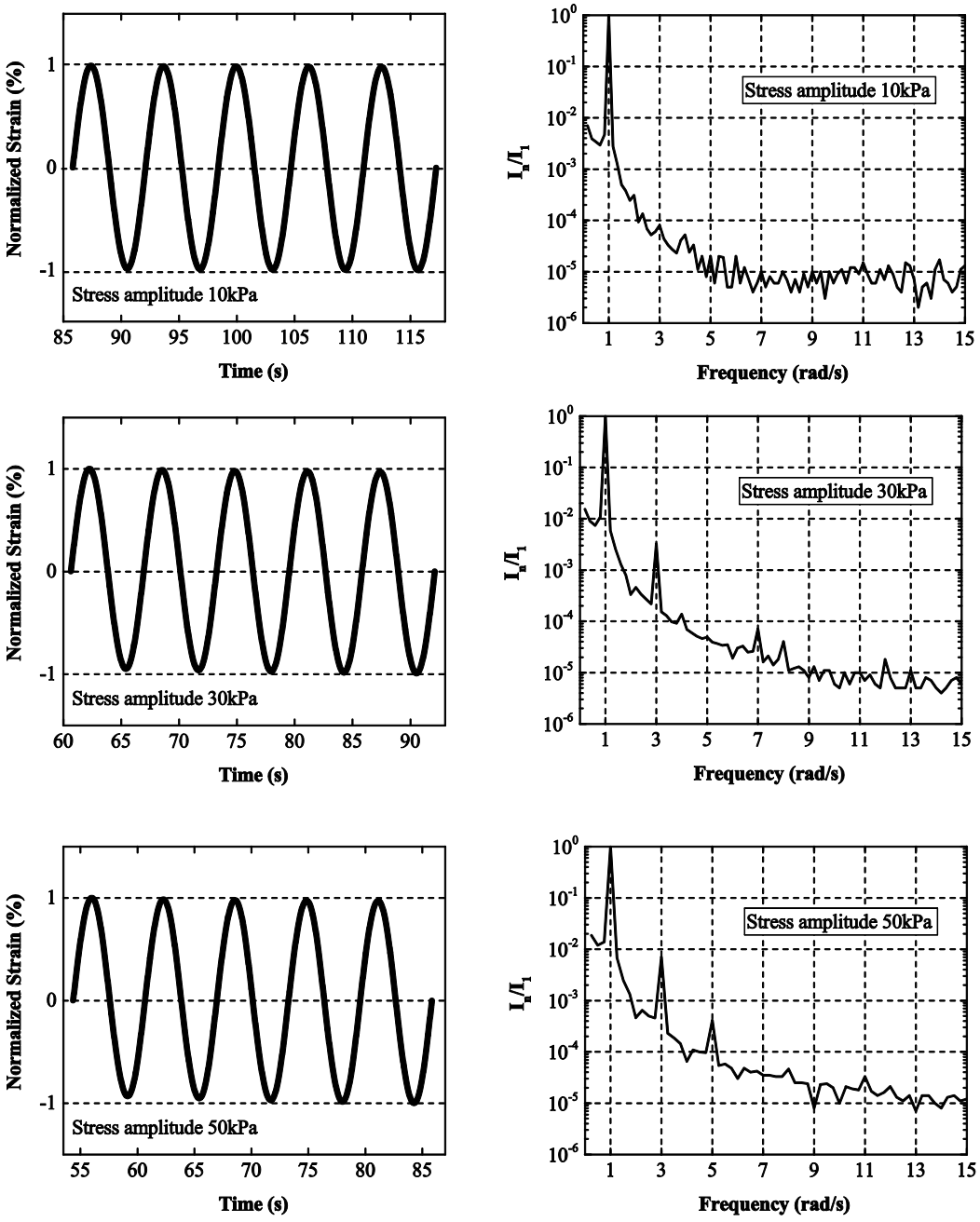

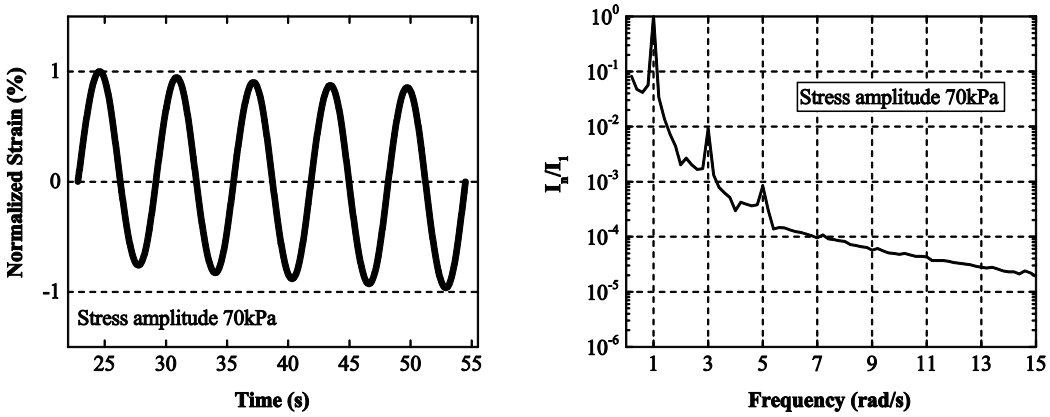


**FIG. 6.** The strain signal (shifted to zero average strain) as a function of time and corresponding Fourier spectra as a function of frequency at various stress amplitude (40kPa, 50kPa, 60kPa, and 70kPa) of bitumen A at 30°C and 1rad/s.

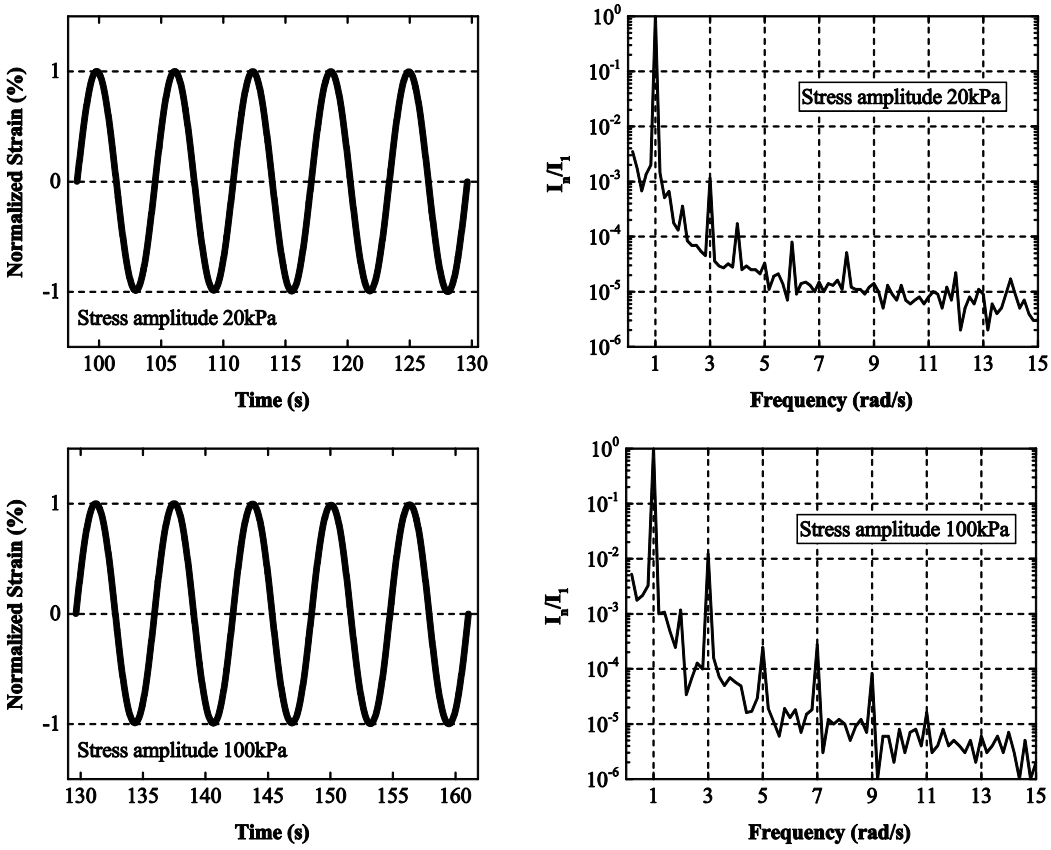

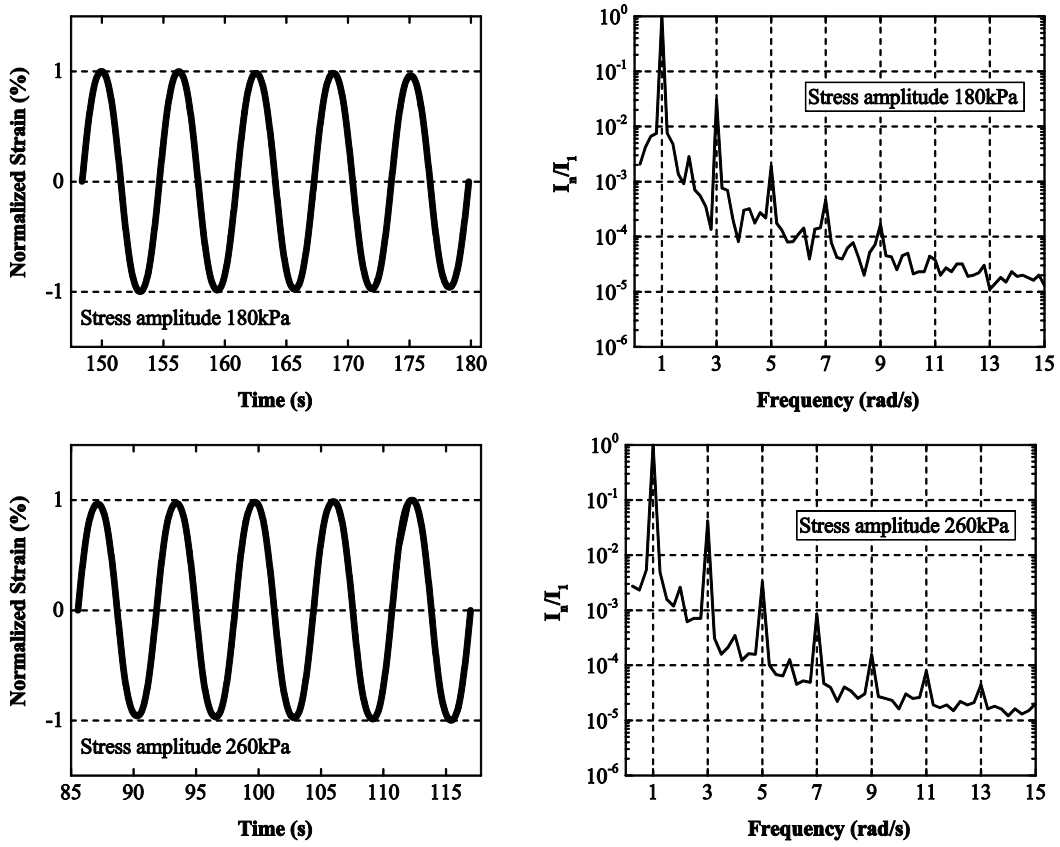


**FIG.7.** The strain signal (shifted to zero average strain) as a function of time and corresponding Fourier spectra as a function of frequency at various stress amplitude (20kPa, 100kPa, 180kPa, and 260kPa) of bitumen B at 30°C and 1rad/s

For the rheometer, the raw torque $M_r$ is the sum of the sample torque $M_s$ and an additional contribution caused by instrument $M_I$ [37, 56, 57] as shown in Eq. (13).

$$M_r(t) = M_s(t) + M_I(t) = \sigma(t)/K_\sigma + I\ddot{\theta}(t) = \sigma(t)/K_\sigma - I\omega^2\theta_0\, sin(\omega t) \quad (13)$$

For small enough frequencies and stress amplitudes, the effect from the instrument inertia can be neglected. But for high frequencies, the instrument effect may dominate over the sample torque. Before analyzing $I_3/I_1$, the $M_{I0}/M_{s0}$ ratios for each test condition were calculated to check the instrument inertia effect (shown in the Supplemental Material). Except 60 rad/s, the $M_{I0}/M_{s0}$ ratios for all the other conditions are lower than 0.03, which means that the effect of instrument inertia can be neglected. For the tests at the frequency of 60 rad/s, the ratios are around 0.10, which means that the results under 60 rad/s are not accurate. So $I_3/I_1$ and $Q$ at 60 rad/s will not be analyzed in the following section.

To analyze the change of relative intensity with stress amplitude, frequency and temperature, the relative third intensity of the studied bitumens under various test conditions are plotted in Figure 8 and Figure 9, and Eq. (14) was used to fit the data.

$$I_3/I_1\,(\sigma_0) = A\left(1 - \frac{1}{1+B{\sigma_0}^C}\right) \quad (14)$$

where the parameter A reflects the maximum intensity of $I_3/I_1$ at high stress amplitude, B is approximately the point of inflection, and the parameter C is the scaling exponent.

It can be seen that C=2 for bitumen A within the MAOS region. C for bitumen B departures from 2 because it contains SBS polymers and crumb rubbers, and based on our study the SBS polymer has lamellar structure. These results are consistent with the reference which states that materials with lamellar or composite like structure departure from C=2 behavior [27].

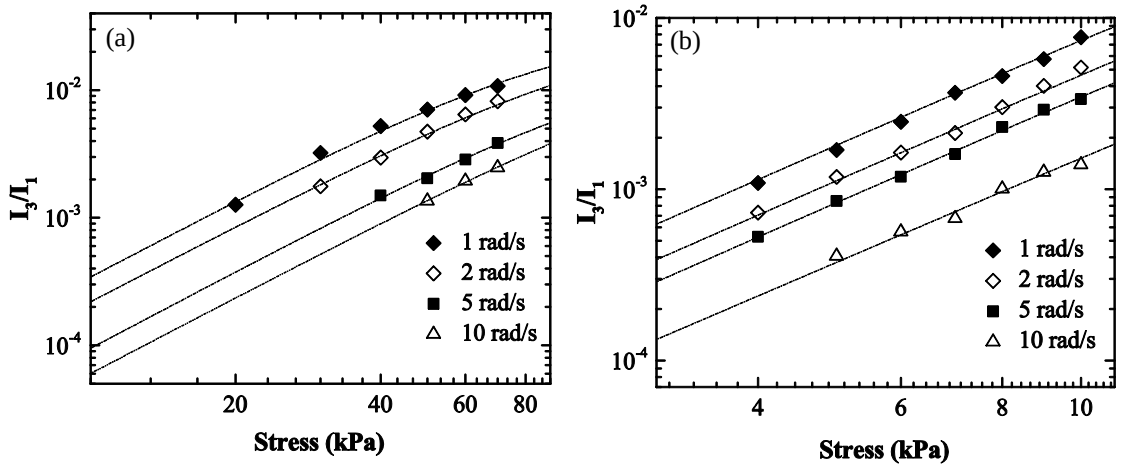


**FIG.8.** The $I_3/I_1$ as a function of stress amplitude of bitumen A at various frequencies and different temperatures: (a) 30°C; (b) 60°C.

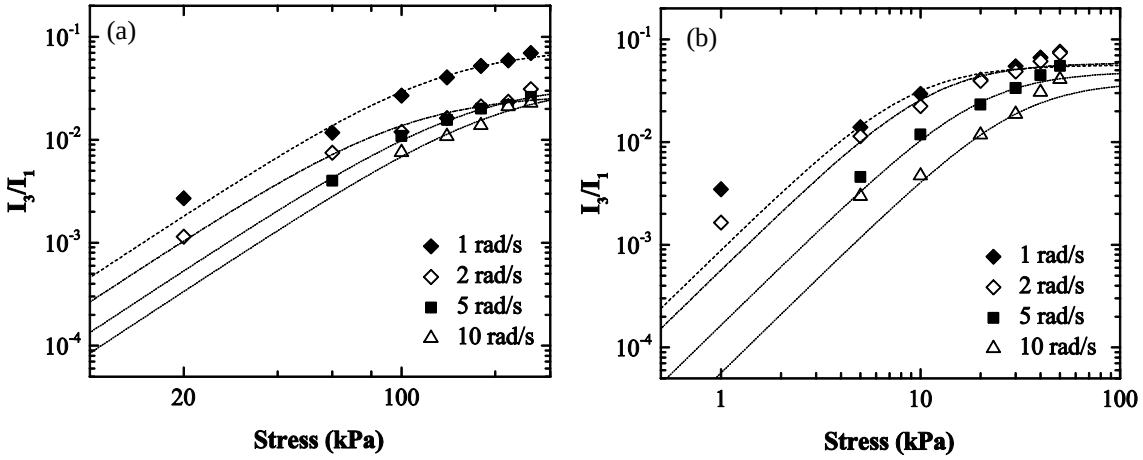


**FIG.9.** The $I_3/I_1$ as a function of stress amplitude of bitumen B at various frequencies and different temperatures: (a) 30°C; (b) 60°C.

Based on the Q parameter theory in the references of Hyun et al.(2009) [58] and Abbasi et al. (2013)[59], the Q parameter under LAOS stress can be described by Eq.(15).The relationships between Q and stress amplitude at various conditions are plotted in Figure 10 and Figure 11. The dotted lines in each figures are the fitting curves by Eq.(15). Because the data is limited, the shapes of the curves among different

conditions are qualitative, however, some trends are evident. It can be seen that $Q$ values decrease with increases in frequency. For the neat bitumen A, the $Q$ value changes little during the test conditions, and it is predicted to decrease with increase in stress based on the modeling results. For the modified bitumen B, the $Q$ value decreases with increases in stress amplitude.

$$logQ = log\frac{I_3/I_1(\sigma_0)}{\sigma_0^2} = logA + logB + Clog\sigma_0 - log(1 + B\sigma_0^C) - 2log\sigma_0 \quad (15)$$

$$Q_0 \equiv \lim_{\sigma_0 \to 0} Q = \lim_{\sigma_0 \to 0} \frac{I_3/I_1(\sigma_0)}{\sigma_0^2} \quad (16)$$

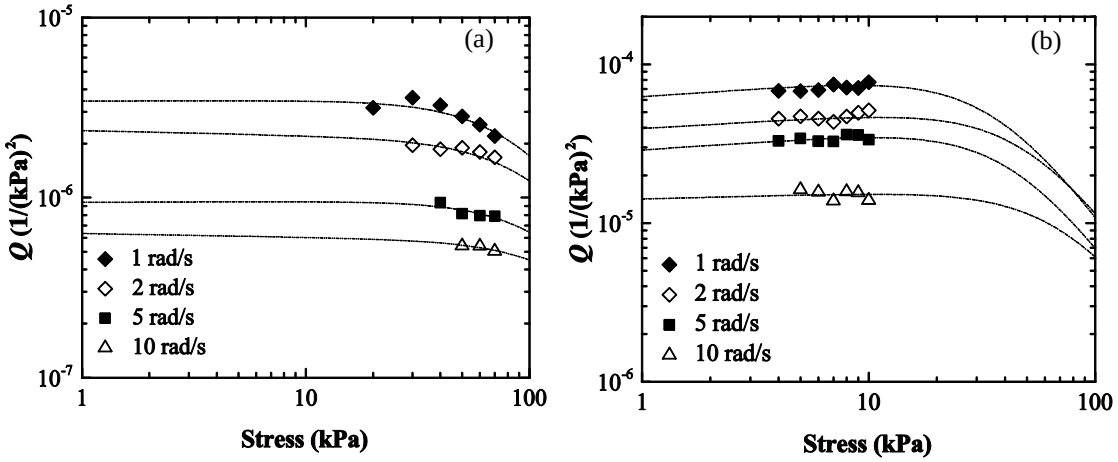


**FIG.10.** $Q = I_3/I_1/\sigma_0^2$ as a function of stress amplitude of bitumen A at various frequencies and different temperatures: (a) 30°C; (b) 60°C.

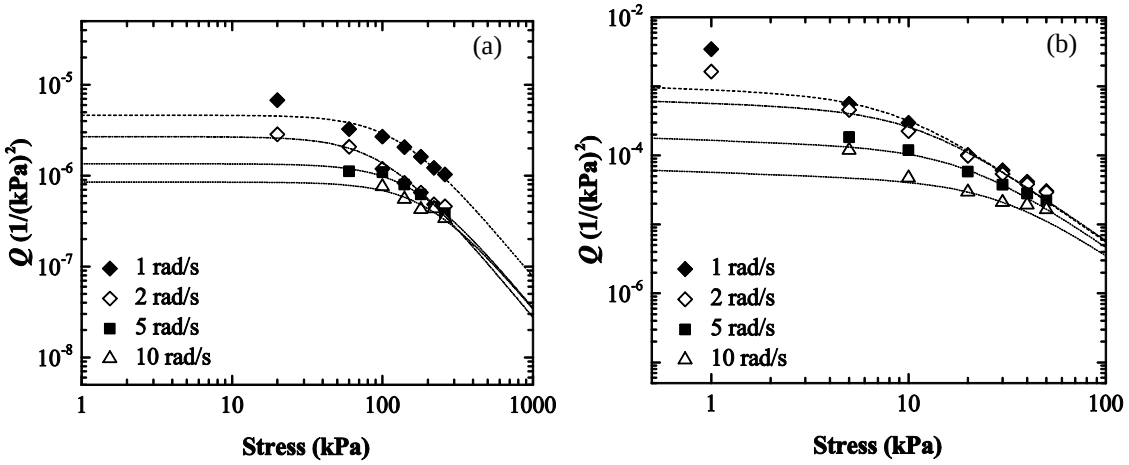


**FIG.11.** $Q = I_3/I_1/\sigma_0^2$ as a function of stress amplitude of bitumen B at various frequencies and different temperatures: (a) 30°C; (b) 60°C.

It can also be seen from Figure 10 and Figure 11 that, at relatively small stress amplitude, Q had a constant value ($Q_0$) that changes with frequency. Based on Eq. (15)

and Eq. (16), $Q_0$=AB (C=2 was used for each condition in order to calculate $Q_0$ value), and the $Q_0$ values for the bitumens are calculated and shown in Figure 12. It shows the trend of $Q_0$ decreasing with frequency and increasing with temperature. The $Q_0$ value of bitumen A is less than that of bitumen B at the same frequency and temperature.

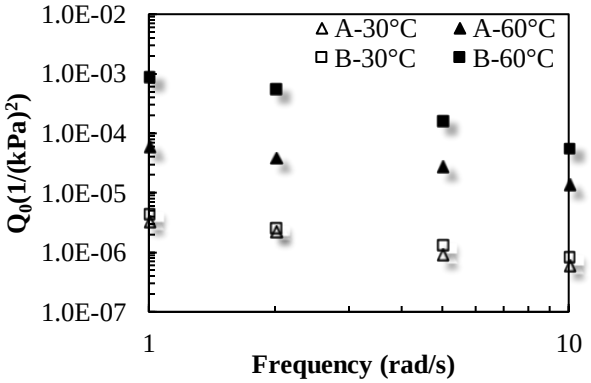


**FIG.12.** $Q_0$ of the studied bitumens at various frequencies and different temperatures.

**B. Strain decomposition**

As described above, the use of Chebyshev polynomials allows decomposition of the strain response into purely elastic and viscous components, represented by $c_n$ and $f_n$. Here we are focusing at $c_3$ and $f_3$ since they are significantly larger than the higher order contributions in all cases.

Examples of strain decomposition with Chebyshev polynominals are presented in Figure 13. Both the elastic [$\gamma(t)$ vs $\tau(t)$] and viscous representation [$\dot{\gamma}(t)$ vs $\tau(t)$] are shown together with the Lissajous curve. For the same bitumen, the shapes of the Lissajous curves are similar at different stress levels. The elastic Lissajous loop is an ellipse as expected, and the nonlinearity of the dotted line [in Figure13 (a),(e),(c) and (g)] becomes more and more obvious with increase in stress level. The viscous Lissajous loop of bitumen A at 30°C is also elliptical but is linear line at 60°C, which shows that bitumen A is viscoelastic at 30°C, and becomes a purely viscous material at 60°C. For bitumen B, the nonlinearity is much more obvious because of a visual inspection of distorted Lissajous loops. The elastic and viscous strain depart from linearity with increasing stress, revealing a rich material response with softening/stiffening and thinning/thickening contributions depending on the frequency as will be discussed below.

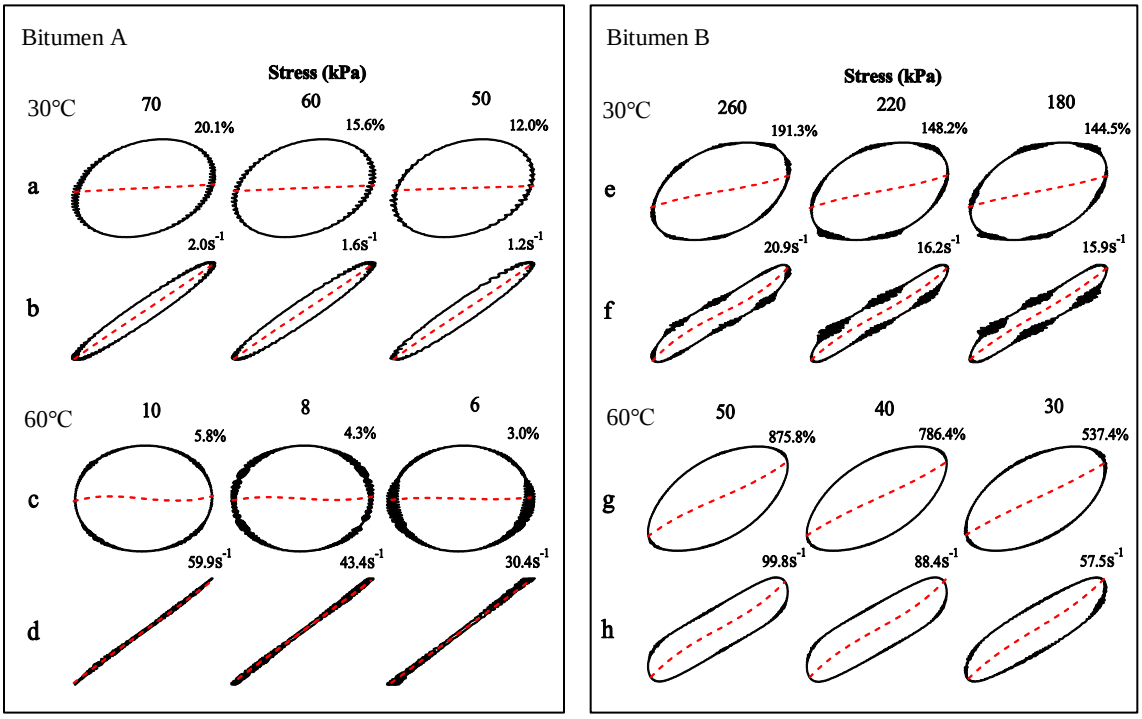


**FIG.13.** Decomposition of shear strain into elastic and viscous part for bitumen A and bitumen B at 10rad/s and different temperatures.

By decomposing the elastic and viscous strain signal into the orthogonal set of Chebyshev polynomial, we may determine quantitatively the stress softening/stiffening and shear thinning/thickening response of the material. Due to the convexity of the third Chebyshev polynomial positive values of $c_3$ result in stress softening of the apparent elastic stress-strain curve, while positive values of $f_3$ result in stress thinning of the apparent plastic strain-rate vs shear stress curve. Conversely, negative values of $c_3$ imply stress stiffening of the elastic material, while negative values of $f_3$ imply stress thickening. Figure 14 and Figure 15 depict $c_3/c_1$ and $f_3/f_1$ as a function of the applied stress at different frequencies and temperatures in the nonlinear regime. With increasing stress, both $c_3/c_1$ and $f_3/f_1$ increase from the overall trend. Both $c_3$ and $f_3$ are positive for bitumen A, which means that bitumen A will reveal stress softening and stress thinning under all the studied test conditions. For bitumen B, $f_3$ is positive under all the conditions, but $c_3$ is negative at some stress and frequency levels when the temperature is 60°C. It means that bitumen B will reveal stress thinning under all the test conditions. But whether it will reveal stress softening or stress stiffening depends on the stress level and frequency. Further more, the stress softening/stress stiffening of the bitumens shown by Figure 15 is consistent with the results shown by Figure 3. It also illustrate that $c_3$ and $f_3$ are useful to reflect the stress softening/stiffening and shear thinning/thickening behavior of viscoelastic materials.

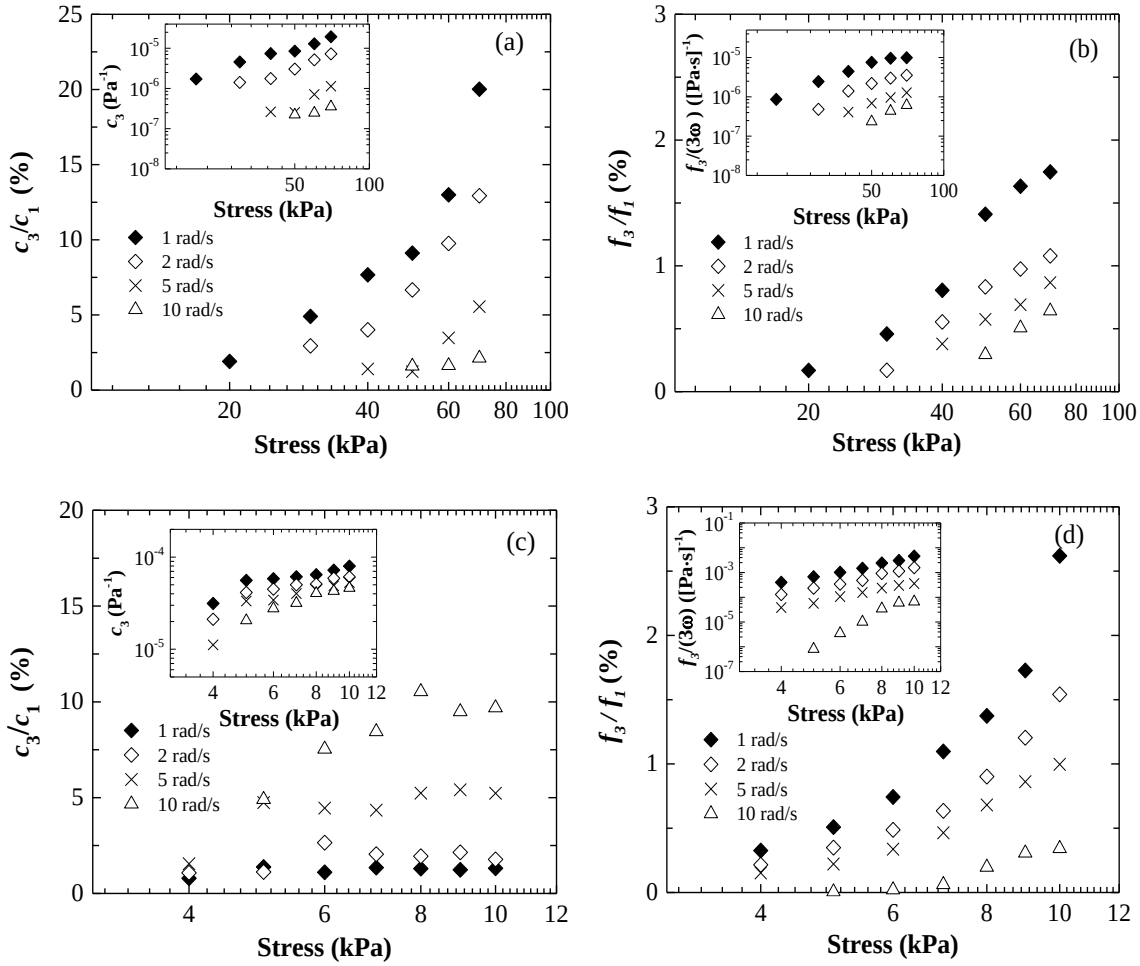


**FIG.14.** Relative third order elastic, $c_3/c_1$, and viscous, $f_3/f_1$ Chebyshev coefficients as a function of stress for bitumen A at different frequencies and temperatures: (a) and (b) 30°C; (c) and (d) 60°C.

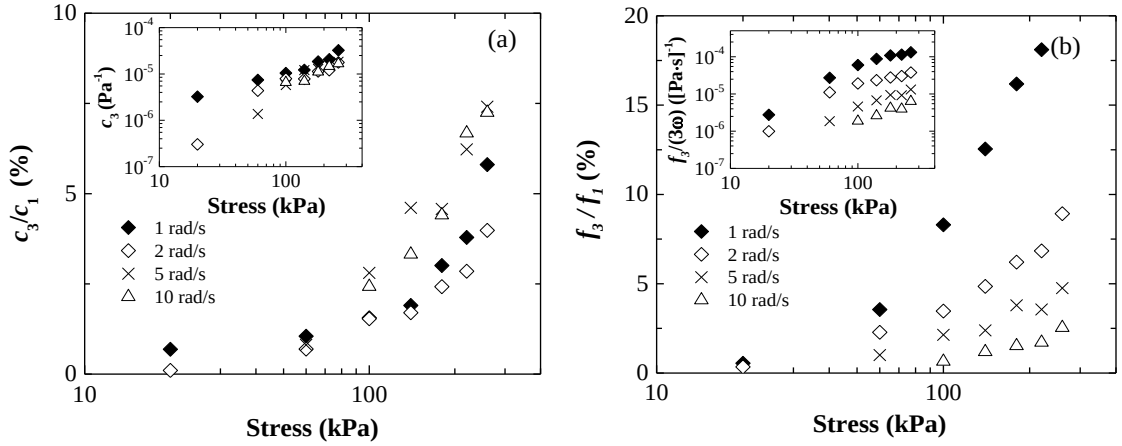

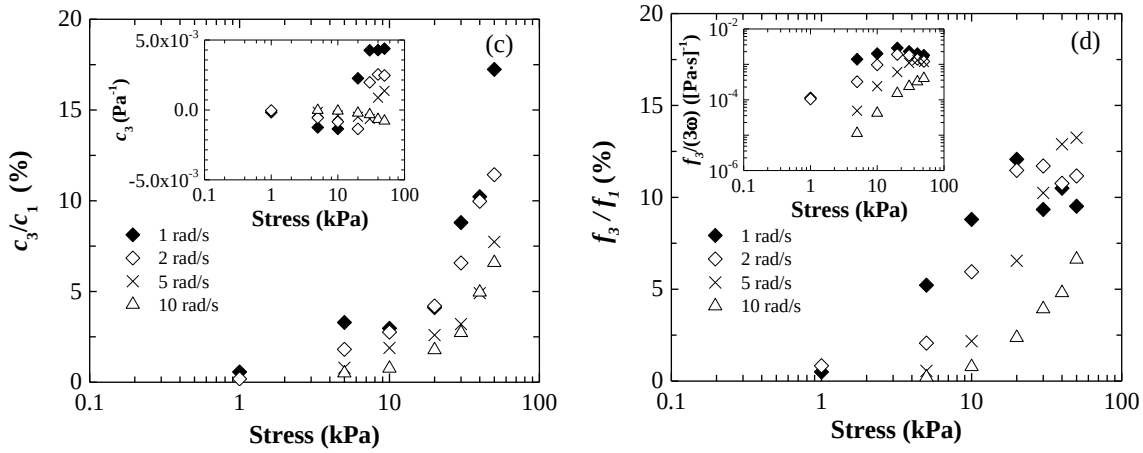


**FIG.15.** Relative third order elastic, $c_3/c_1$, and viscous, $f_3/f_1$ Chebyshev coefficients as a function of stress for bitumen B at different frequencies and temperatures: (a) and (b) 30°C; (c) and (d) 60°C.

## Ⅴ. CONCLUSIONS

We have presented a protocol to obtain the nonlinear rheological behavior of bitumen under LAOS stress. Both FT-rheology and stress decomposition methods are applied to analyze the nonlinear rheological behavior of one kind of neat bitumen and one kind of modified bitumen. Distinct differences are observed between the neat and modified bitumen. Our results show that the relative intensity of the nonlinear parameter of bitumen increases with increase in stress and decrease in frequency. Furthermore the nonlinearity of modified bitumen B is much more significant than neat bitumen A. The relationship between $I_3/I_1$ and stress amplitude obeys a sigmoidal function. The Q parameter, which equals to $\frac{I_3/I_1(\sigma_0)}{\sigma_0^2}$, is a nonlinear material property that identifies property differences between neat and modified bitumen. The intrinsic nonlinearity $Q_0$ decreases with increase in frequency and decrease in temperature. The $Q_0$ value of bitumen A is less than that of bitumen B at the same frequency and temperature, which also slows that the nonlinearity of bitumen B is more obvious than bitumen A. The strain decomposition results show that bitumen A is viscoelastic material at 30°C and pure viscous at 60°C; bitumen B is viscoelastic at both 30°C and 60°C. Analysis of the Chebyshev polynomial shows that bitumen A exhibits stress softening and stress thinning under all the studied test conditions. Bitumen B exhibits stress softening and stress thinning at 30°C, but stress stiffening at some stress and frequency levels when the temperature is 60°C. These results that illustrate useful information distinguishing bitumen samples can be rapidly and accurately obtained from LAOS stress measurements, suggesting it is meaningful to perform further studies of the nonlinear rheological characteristics of bitumen under LAOS, especially with respect to identifying the nonlinear constitutive model that can predict the material behavior. Further more, it can

provide references for study the fatigue performance of bitumen under LAOS in the next research step.

## SUPPLEMENTAL MATERIAL

See supplemental material for the generalized Kelvin model parameters for bitumen A and bitumen B at 30°C and 60°C, and $M_{I0}/M_{s0}$ ratios under all the studied conditions.


## ACKNOWLEDGEMENTS

This study was sponsored by the National Natural Science Foundation of China (51478153 and 51778195) and China Scholarship Council (CSC). The author extend their thanks to Paul M. Mwasame for help with the test protocol and discussions about the Lissajous curves, Simon A. Rogers for useful advice concerning the LAOS interpretation and further research, as well as B. Shane Underwood and Akshay Gundla for providing the studied bitumen.


## Appendix

All the shift factors of the strains for bitumen A and bitumen B under different conditions are summarized in Table Ⅳ and Table Ⅴ. It can be seen from the tables that there is no obvious trends of the shift factors, except that the shift factors at 60 ℃ are larger than the factors at 30 ℃

**TABLE Ⅳ.** The shift factors of bitumen A under different conditions.

| Frequency (rad/s) | | 1 | 2 | 5 | 10 | 60 |
|---|---|---|---|---|---|---|
| Shift factor at 30 °C (%) | 10 kPa | 4.8 | 1.5 | 0.6 | 0.2 | -0.1 |
| | 20 kPa | 8.1 | 3.0 | 1.4 | 0.9 | -0.2 |
| | 30 kPa | 10.4 | 5.2 | 2.5 | 1.5 | -0.3 |
| | 40 kPa | 1.4 | 5.3 | 3.0 | 2.0 | -0.2 |
| | 50 kPa | -27.4 | 4.7 | 3.6 | 2.4 | -0.1 |
| | 60 kPa | -5.1 | -6.7 | 2.2 | 1.2 | 0 |
| | 70 kPa | -18.8 | -4.9 | -0.6 | -0.2 | -0.2 |
| Shift factor at 60 °C (%) | 4 kPa | -366.9 | -40.3 | 57.4 | 0 | 0.2 |
| | 5 kPa | 765.3 | -30.6 | 135.8 | 21.1 | -1.2 |
| | 6 kPa | 1468.3 | -7.6 | -3.2 | 6.2 | 2.1 |
| | 7 kPa | 57.0 | -899.3 | 0 | -2.1 | 19.0 |
| | 8 kPa | -12.9 | -276.2 | -124.8 | 5.6 | 3.8 |
| | 9 kPa | -84.5 | -206.8 | 61.8 | 34.3 | 0.2 |
| | 10 kPa | 446.3 | -125.2 | -58.3 | 81.3 | 31.1 |

**TABLE Ⅴ.** The shift factors of bitumen B under different conditions.

| Frequency (rad/s) | | 1 | 2 | 5 | 10 | 60 |
|---|---|---|---|---|---|---|
| Shift factor at 30 °C (%) | 20 kPa | 4.9 | 3.5 | 1.0 | 0.5 | -0.2 |
| | 60 kPa | -0.1 | 0 | -6.3 | -0.2 | 0 |
| | 100 kPa | -3.4 | -4.6 | 6.2 | -0.3 | -0.6 |
| | 140 kPa | 6.4 | 0.1 | -2.4 | 1.7 | 0.4 |
| | 180 kPa | 10.0 | 4.8 | -4.6 | 5.0 | 2.5 |
| | 220 kPa | 22.0 | 12.5 | 6.2 | -8.1 | 2.2 |
| | 260 kPa | 37.5 | 0.6 | 1.9 | -3.1 | 0.6 |
| Shift factor at 60 °C (%) | 1 kPa | 4.5 | 2.8 | 4.3 | 1.5 | -0.1 |
| | 5 kPa | 42.7 | 44.5 | 8.1 | 5.2 | 0.1 |
| | 10 kPa | 70.8 | 67.8 | -25.7 | -0.8 | 1.7 |
| | 20 kPa | -121.1 | 64.0 | 10.9 | -4.5 | -5.6 |
| | 30 kPa | 350.5 | 35.3 | 3.5 | -20.8 | -10.5 |
| | 40 kPa | -1005.9 | -328.2 | 145.1 | -173.6 | -16.6 |
| | 50 kPa | 1202.0 | 723.6 | 17.1 | -91.7 | 286.5 |

**References**


[1] Vinogradov, G.V., A.I. Isayev, V.A.Zolotarev, and E.A. Verebskaya, "Rheological properties of road bitumens,"Rheol. Acta **16**, 266-281(1977).

[2] Cheung, C.Y., and D.Cebon, "Experimental study of pure bitumens in tension, compression, and shear, " J. Rheol. **41**(1), 45-73(1997).

[3] García-Morales, M., P. Partal, F.J. Navarro, F. Martínez-Boza, M.R. Mackley, and C. Gallegos, "The rheology of recycled EVA/LDPE modified bitumen," Rheol. Acta **43**, 482-490(2004).

[4] Behzadfar, E., and S.G. Hatzikiriakos, "Rheology of bitumen: effects of temperature, pressure, $CO_2$ concentration and shear rate," Fuel **116**, 578-587(2014).

[5] Lesueur, D., J.F.G. Claudy, J.M.Letoffe, J.P. Planche, and D. Martin, "A structure-related model to describe asphalt linear viscoelasticity," J. Rheol. **40**, 813-836(1996).

[6] Lesueur, D., J.F.G. Claudy, J.M.Letoffe, D. Martin, and J.P. Planche, "Polymer modified asphalts as viscoelastic emulsions," J. Rheol. **42**,1059-1074(1998).

[7] Lesueur, D., "The colloidal structure of bitumen: consequences on the rheology and on the mechanisms of bitumen modification," Advances in Colloid and Interface Science **145**, 42-82(2009).

[8] Partal, P., F. Mart í nez-Boza, B. Conde, and C. Gallegos, "Rheological characterization of synthetic binders and unmodified bitumens," Fuel **78**,

1-10(1999).

[9] García-Morales, M., P. Partal, F.J. Navarro, and C. Gallegos, "Effect of waste polymer addition on the rheology of modified bitumen," Fuel **85**, 936-943(2006).

[10] Machemehl, R., and C.E. Lee. Dynamic traffic loading of pavements, Research report 160-1F, Center for Highway Reseasrch, The University of Texas at Austin, 1974.

[11] Stastna, J., L. Zanzotto, and K. Ho, "Fractional complex modulus manifested in asphalts," Rheol Acta **33**, 344-354(1994).

[12] Zanzotto, L., J. Stastna, and K. Ho, "Characterization of regular and modified bitumens via their complex moduli, " J. Applied. Polym. Sci. **59**, 1897-1905(1996).

[13] Williams, M.L., R.F. Landel, and J.D. Ferry, "The temperature dependence of relaxation mechanisms in amorphous polymers and other glass-forming liquids,"J.Am. Chem. Soc. **77**(14), 3701-3707(1955).

[14] Arrhenius, S.A., "Über die dissociationswärme und den Einfluß der temperatur auf den dissociationsgrad der electrolyte," Z.Phys. Chem. **4**, 96-116(1889).

[15] Mastrofini, D., and M. Scarsella, "The application of rheology to the evaluation of bitumen ageing," Fuel **79**, 1005-1015(2000).

[16] Christensen D.W., and D.A. Anderson, "Interpretation of dynamic mechanical test data for paving grade asphalt cements," J. Assoc. Asphalt Paving Techn. **61**, 67-98(1992).

[17] Dickinson E.J., F.H. Gaskins, W. Philippoff, and E. Thelen, "The rheology of asphalt. Ⅲ Dynamic mechanical properties of asphalt," Trans. Soc. Rheol. **18**, 591-606(1974).

[18] Duffrene, L., R. Gy, H. Burlet, and R. Piques, "Multiaxial linear viscoelastic behavior of a soda-lime-silica glass based on a generalized Maxwell model" J. Rheol. **41**, 1021-1038(1997).

[19] Maestro, A., C. Gonzalez, and J.M. Gutierrez, "Rheological behavior of hydrophobically modified hydroxyethyl cellulose solutions: A linear viscoelastic model" J. Rheol. **46**, 127-142(2002).

[20] Reyes, M., I. Kazatchkov, J. Stastna, and L. Zanzotto, "Modeling of repeated creep and recovery experiments in asphalt binders." Transport. Res. Rec. **2126**, 63-72(2009).

[21] Mun, S., and G. Zi, "Modeling the viscoelastic function of asphalt concrete using a spectrum method," Mech. Time-Depend. Mater **14**,191-202(2010).

[22] Chang K., and J. Meegoda, "Micromechanical simulation of hot mix asphalt, " J. Eng. Mech. **123**(5), 495-503(1997).

[23] Huet, C., "Etude par une me´thode d'impe´dance du comportement viscoe´lastique des mate´riaux hydro-carbones," Thesis (PhD). Faculte´ des Sciences de Paris, France (1963).

[24] Olard, F., and H. D. Benedetto, "The "DBN" model: A thermo-visco-elasto-plastic

approach for pavement behavior modeling," J. Assoc. Asphalt Paving Technol.**74**, 791-828(2005).

[25] Bahia, H.U., H. Zhai, K. Bonnetti, and S. Kose, "Non-linear viscoelastic and fatigue properties of asphalt binders," J. of Assoc. of Asphalt Paving Technol. **68**,1-34(1999).

[26] Conte, T., and M. Chaouche, "Rheological behavior of cement pastes under Large Amplitude Oscillatory Shear," Cement Concrete Res. **89**,332-344(2016).

[27] Hyun, K., M. Wilhelm, C.O. Klein, K.S. Cho, J.G. Nam, K.H. Ahn, S.J. Lee, R.H. Ewoldt, and G.H. Mckinley, "A review of nonlinear oscillatory shear tests: Analysis and application of large amplitude oscillatory shear (LAOS)," Prog. Polym. Sci. **36**,1697-1753(2011).

[28] Lee, S.H., H.Y. Song, and K.H.H.Lee, "Nonlinearity from FT-rheology for liquid crystal 8CB under large amplitude oscillatory shear (LAOS) flow," J. Rheol. **59**,1-19(2015).

[29] Rogers, S.A., M.P. Lettings, "A sequence of physical processes determined and quantified in large-amplitude oscillatory shear (LAOS): Application to theoretical nonlinear models," J. Rheol. **56**,1-25(2012).

[30] Padmarekha, A., K. Chockalingam, U.Saravanan, A.P. Deshpande, and J.M. Krishnan, "Large amplitude oscillatory shear of unmodified and modified bitumen," Road Mater. Pavement **14**,12-24(2013).

[31] Farrar, M.J., J.P. Planche, A.O. Cookman, and S. Salmans, "Asphalt binder large amplitude oscillatory shear," Western Research Institute Binder ETG meeting, Baton Rouge, LA, Sept.16, 2014.

[32] Jorshari, K., J. Stastna, and L. Zanzotto, "Large amplitude oscillations in asphalt," Journal of Applied Asphalt Binder Technology, **1**,51-71(2001).

[33] Stastna, J., K. Jorshari, and L. Zanzotto, "Nonlinear dynamic moduli in asphalt," Mater. Struct. **35**, 59-63(2002).

[34] González, E., L.M.B. Costa, H.M.R.D. Silva, and L. Hilliou, "Rheological characterization of EVA and HDPE polymer modified bitumens under larger deformation at 20°C, " Constr. Build. Mater. **112**,756-764(2016).

[35] E.Masad, V.T.F.Castelo Branco, D.N.Little, and R.Lytton. "A unified method for the analysis of controlled-strain and controlled-stress fatigue testing," Int. J. Eng. **9**,233-246(2008).

[36] Läuger, J., and H. Stettin. "Differences between stress and strain control in the non-linear behavior of complex fluids," Rheol. Acta. **49**(9),909-930(2010).

[37] Dimitriou, C.J., R.H. Ewoldt, and G.H.McKinley, "Describing and prescribing the constitutive response of yield stress fluids using large amplitude oscillatory shear stress (LAOStress)," J. Rheol. **57**(1), 27-70(2013).

[38] Sörensen,A. and B. Wichert, "Asphalt and bitumen," Ullmann's Encyclopedia of Industrial Chemistry, 2009.

[39] Robertson, R.E., J. F. Branthaver, P. M. Harnsberger, et al. Fundamental properties

of asphalts and modified asphalts, volume I: Interpretive report, 2001.
[40] Yu, X., M. Zaumanis, S.D. Santos, and L.D. Poulikakos, "Rheological, microscopic, and chemical characterization of the rejuvenating effect on asphalt binders," Fuel **135**,162-171(2014).
[41] Mewis, J., and N.J. Wagner. "Colloidal suspension rheology," Cambridge University Press, 2012.
[42] Shan, L.Y., Y.Q. Tan, H. Zhang, and Y.N. Xu, "Analysis of linear viscoelastic response function model for asphalt binders," J. Mater. Civil Eng. **28**(6), 04016010(2016).
[43] Ewoldt, R.H., P. Winter, J. Maxey, and G.H. McKinley, "Large amplitude oscillatory shear of pseudoplastic and elastoviscoplastic materials, " Rheol Acta. **49**,191-212(2010).
[44] Wilhelm, M., D. Maring, and H.W. Spiess. "Fourier-transform rheology," Rheol. Acta. **37**,399-405(1998).
[45] Wilhelm, M., P.Reinheimer, and M. Ortseifer. "High sensitivity Fourier-transform rheology," Rheol. Acta. **38**,349-356(1999).
[46] Ewoldt, R.H., "Defining nonlinear rheological material functions for oscillatory shear," J.Rheol. **57**(1), 177-195(2013).
[47] Hyun, K., E.S. Baik, K.H. Ahn, S.J. Lee, and M. Koyama, "Fourier-transform rheology under medium amplitude oscillatory shear for linear and branched polymer melts," J. Rheol. **51**,1319-1342(2007).
[48] Hyun, K., and M. Wilhelm, "Establishing a new mechanical nonlinear coefficient *Q* from FT-Rheology: first investigation on entangled linear and comb polymer model systems," Macromolecules **42**,411-422(2009).
[49] Pearson, D.S., and W.E. Rochefort, "Behavior of concentrated polystyrene solution in large-amplitude oscillatory shear fields," J.Polym. Sci. **20**, 83-98(1982).
[50] Helfand, E., and D.S. Pearson, "Calculation of the non-linear stress of polymers in oscillatory shear fields," J. Polym. Sci., Polym.Phys.Ed. **20**, 1249-1258(1982).
[51] Hyun, K., K.H. Ahn, S. J. Lee, M. Sugimoto, and K. Koyama, "Degree of branching of polypropylene measured from Fourier-transform rheology," Rheol. Acta. **46**, 123-129(2006).
[52] Wihelm, M., "Fourier-transform Rheology," Macromol. Mater. Eng. **287**,83-105(2002).
[53] Ewoldt, R.H., A.E. Hosoi, and G.H. McKinley, "New measures for characterizing nonlinear viscoelasticity in large amplitude oscillatory shear," J. Rheol. **52**, 1427-1458 (2008).
[54] Renou, F., J. Stellbrink, and G. Petekidis, "Yielding process in a colloidal glass of soft star-like micelles under large amplitude oscillatory shear (LAOS)," J. Rheol. **54**(6), 1219-1242 (2010).
[55] Rogers, S.A., and D.Vlassopoulos, "Frieze group analysis of asymmetric response to large-amplitude oscillatory shear," J. Rheol. **54**(4),859-880(2010).

[56] Frank A. “Measuring structure of low viscosity fluids in oscillation using rheometers with and without a separate torque transducer,” Ann Trans Nord Rheol Soc 11: RH090, 2003.

[57] Merger, D., M. Wilhelm. “Instrinsic nonlinearity from LAOStrain-experiments on various strain- and stress-controlled rheometers: a quantitative comparison,” Rheol Acta. **53**, 621-634(2014).

[58] Hyun, K. and M. Wilhelm, “Establishing a new mechanical nonlinear coefficient *Q* from FT-Rheology: first investigation of entangled linear and comb polymer model systems,” Macromolecules **42**(1),411-422(2009).

[59] Abbasi, M., N.G. Ebrahimi, and M. Wihelm, “Investigation of the rheological behavior of industrial tubular and autoclave LDPEs under SAOS, LAOS, transient shear, and elongational flows compared with predictions from the MSF theory,” J. Rheol. **57**(6),1693-1714(2013).